

Strontium and simvastatin dual loaded hydroxyapatite microspheres reinforced poly(ϵ -caprolactone) scaffolds promote vascularized bone regeneration

Gen Li¹, Yubao Li¹, Xianhui Zhang², Pengfei Gao², Xue Xia¹, Shiqi Xiao¹, Jing Wen¹, Tao Guo³, Weihu Yang^{2*} and Jidong Li^{1*}

¹Research Center for Nano-Biomaterials, Analytical and Testing Center, Sichuan University, Chengdu 610064, China

²Key Laboratory of Biorheological Science and Technology, Ministry of Education College of Bioengineering, Chongqing University, Chongqing 400044, China

³Department of Orthopaedics, Guizhou Provincial People's hospital, Guiyang 550002, China

*Corresponding author: Jidong Li, E-mail: nic1979@scu.edu.cn Tel: +86 028 85418178;

Weihu Yang, E-mail: yangweihu@cqu.edu.cn Tel: +86 023 65102507

Materials and methods

Preparation of calibration curve of SIM

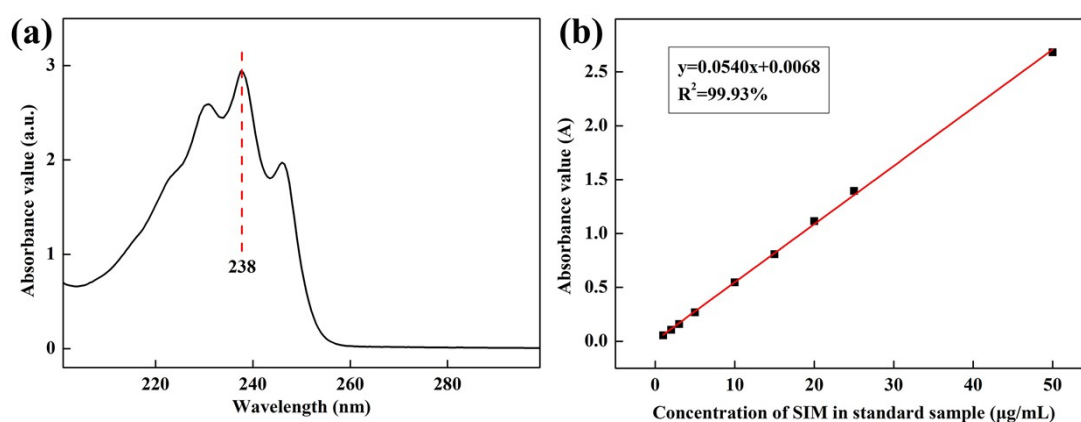


Fig. S1. (a) UV spectrum and (b) calibration curve at 238 nm of SIM. The equation of linear regression was $y = 0.0540x + 0.0068$, $R^2 = 0.9993$, in this experiment.

UV scanning from 100 to 1,000 nm was used to identify the absorption peak of SIM shown in Fig. S1. It was identified that the absorbance of SIM solution was greatly affected by its concentration at 238 nm. The standard absorption curve of SIM was calculated according to the absorbance of samples with known SIM concentrations at 238 nm. Then SIM content in the collected buffer was calculated according to the standard absorption curve of SIM in the same buffer.

Collagen secretion assay

BMSCs were conditionally cultured in the extracts of different scaffold for 14 days. Firstly, Sirius red was executed to stain the various samples for qualitatively observation the collagen secretion. Then, 1 mM of NaOH solution was performed to treat stained samples for quantitatively assay. At last, the collagen secretion amount was detected by at the OD value 540 nm.

Mineralization assay

BMSCs was conditionally cultured on scaffolds for 21 days. Firstly, Alizarin red working solution (pH 4.1) was applied to stain the various samples for 30 min for qualitatively observation. Then, acetic acid solution (10% v/v) and ammonia solution (10% v/v) were used to treat stained samples. Finally, the mineralization amount of BMSCs was detected at the OD value 405 nm.

Table S1 Primer sequence used for RT-PCR gene expression test

mRNA	Forward primer	Reverse primer
GAPDH	AGGTCGGTGTGAACGGATTTG	TGTAGACCATGTAGTTGAGGTCA
β -actin	GAAGATCAAGATCATTGCTCC	TACTCCTGCTTGCTGATCCA
Col I	GCTCCTCTTAGGGGCCACT	CCACGTCTCACCATTGGGG
OPG	ACCCAGAAACTGGTCATCAGC	CTGCAATACACACACTCATCACT
OPN	AGCAAGAAACTCTTCCAAGCAA	GTGAGATTTCGTCAGATTCATCCG
Runx2	AAATGCCTCCGCTGTTATGAA	GCTCCGGCCCCACAAATCT
VEGF	CAGGACCATGAACTTTCTGC	CCTCAGTGGGCACACACTCC
CXCR4	TACCTCGCTATTGTCCACGC	GTGCACGATGCTCTCGAAGT
HIF-1 α	CCTACTATGTCGCTTTCTTG	TGTATGGGAGCATTAAC TTCAC
SDF-1	GTCCACCTCGGTGTCCTCTT	GGGCACAGTTTGGAGTGTTG
Pecam1	CACAACAAACAAGCTAGCAAGA	TTTGGCTGCAACTATTAAGGTG
Vegfa	TAGAGTACATCTTCAAGCCGTC	CTTTCTTTGGTCTGCATTCACA
Tnfrsf11a	CTGAAAAGCACCTGACAAAAGA	CTGTGTAGCCATCTGTTGAGTT
Ocstamp	CTGCGTTTCGACAATATCTACG	TACTAAGAGCAATGCCAGTAGC

Results and discussion

Design and characterization of the microscopes

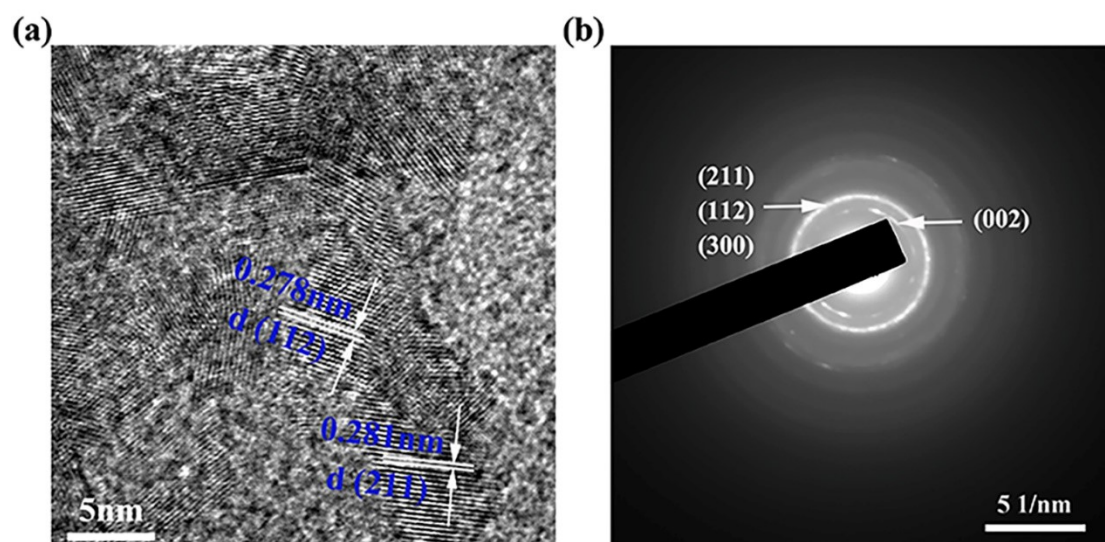


Fig. S2. HRTEM and SAED pattern of SrMHA-SIM

High resolution transmission electron microscope (HRTEM) image and selected area electron diffraction (SAED) patterns of the synthesized SrMHA-SIM was presented in Fig S2. The HRTEM image shows a lattice distance of 0.281nm, identifying the (211) planes of single-crystal HA. The d-spacings of the (211), (112) and (300) planes nearly overlap with each other giving rise to a combined ring¹. Spacing and angles of the lattice fringes, in the two cases, can consistently be assigned to the structure of hydroxyapatite.

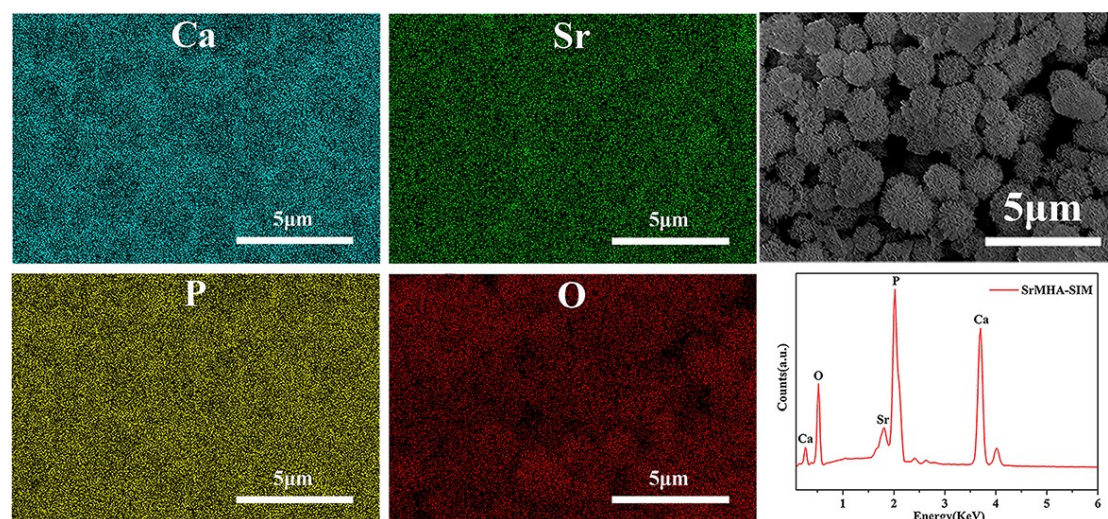


Fig. S3. Mapping and spectrum of the SrMHA-SIM microspheres

Table S2 Fiber size, pore size and porosity of different scaffolds

Samples	Fiber size (μm)	Pore size (μm)	Porosity (%)
PH	543.25 \pm 15.84	266.75 \pm 15.01	68.39 \pm 1.41
PSrH	551.69 \pm 21.20	253.82 \pm 5.35	66.88 \pm 1.61
PHS1	483.77 \pm 13.60	300.88 \pm 3.96	69.88 \pm 0.40
PHS5	511.65 \pm 16.64	287.02 \pm 11.24	65.56 \pm 1.83
PSrHS1	495.81 \pm 36.04	278.45 \pm 6.19	69.59 \pm 0.65
PSrHS5	480.24 \pm 42.01	296.03 \pm 7.12	66.39 \pm 0.74

Design and characterization of the scaffolds

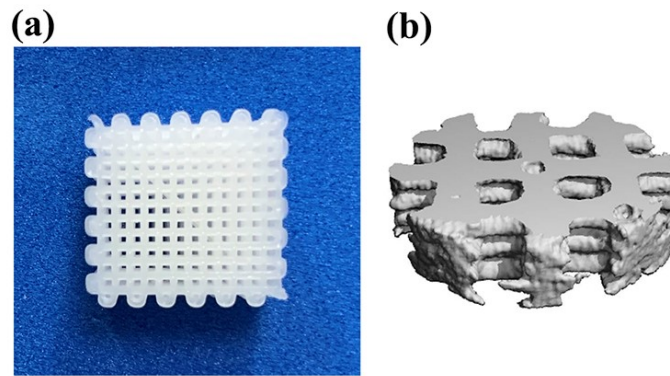


Fig. S4. (a) Digital images and (b) representative micro-CT images of printed PSrHS5 scaffolds

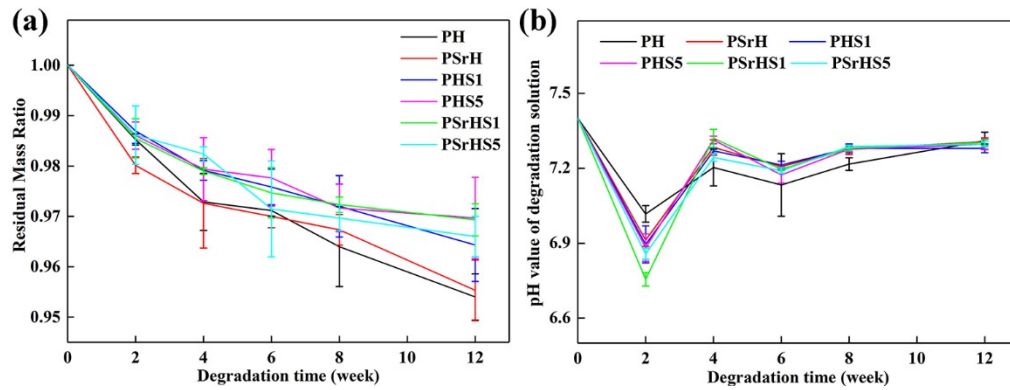


Fig. S5. (a) Degradation and (b) pH value of degradation solution of the different scaffolds in vitro.

The data are presented as the mean \pm SD (n = 3)

In order to investigate the effect of PCL, Sr, and SIM components on the degradation behavior of the composite scaffolds, the weight loss of scaffolds after immersing in PBS and the pH value of degradation solutions were measured (Fig. S5). The weight loss percentage for the all scaffolds was less than 5% at 12 weeks. In addition, the degradation of PCL-based scaffolds induce the slight decrease in pH value of the degradation solutions (Fig. S5b), which is mainly due to the production of acid degradation products². Because of the slow degradation rate, PCL is preferable to match the rate of bone tissue ingrowth or complete healing³.

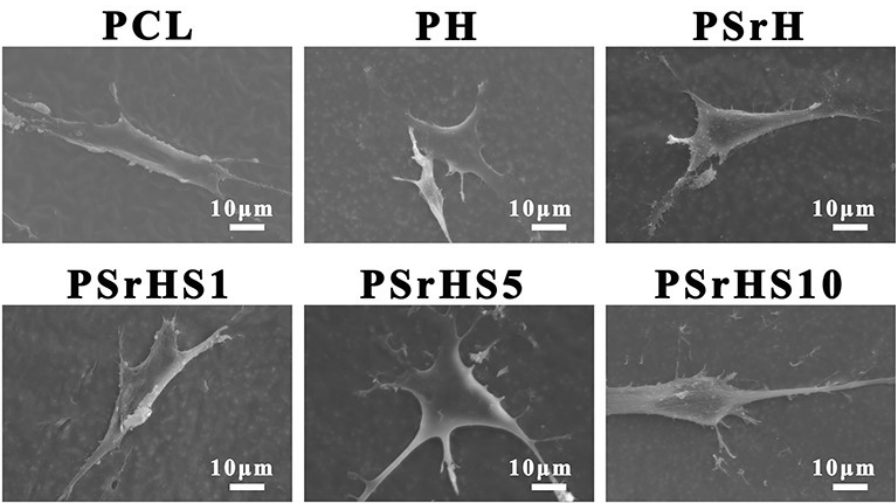


Fig. S6. Cell morphology of BMSCs cells cultured on different scaffolds for 3 days

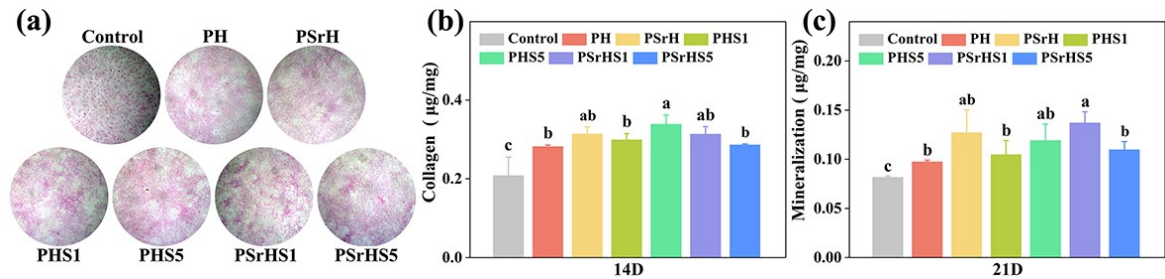


Fig. S7 (a) Representative staining images of collagen expression of BMSCs cultured at 14 days, (b) Quantitative analysis of collagen expression of BMSCs cultured at 14 days and (c) mineralization of BMSCs cultured at 21 days. The data are presented as the mean \pm SD (n = 3)

The expression of collagen and mineralization of cultured BMSCs in the extracts of different scaffolds

were further studied (Fig. S7). The results revealed that collagen expression and mineralization in all scaffold groups were significantly higher than those in the control group. The collagen expression and mineralization of PSrH, PSrHS1 and PHS5 were higher than those of other groups. It's worth noting, the collagen expression of PSrHS5 group was significantly lower than that of PHS5, and the mineralization of PSrHS5 was significantly lower than that of PSrHS1. Although both Sr and SIM can activate osteogenic differentiation related factors such as RUNX2 in BMSCs⁴. The lower collagen and mineralization of PSrHS5 group may be related to the higher SIM content released by the PSrHS5 scaffold, resulting in a lower number of cells in this group.

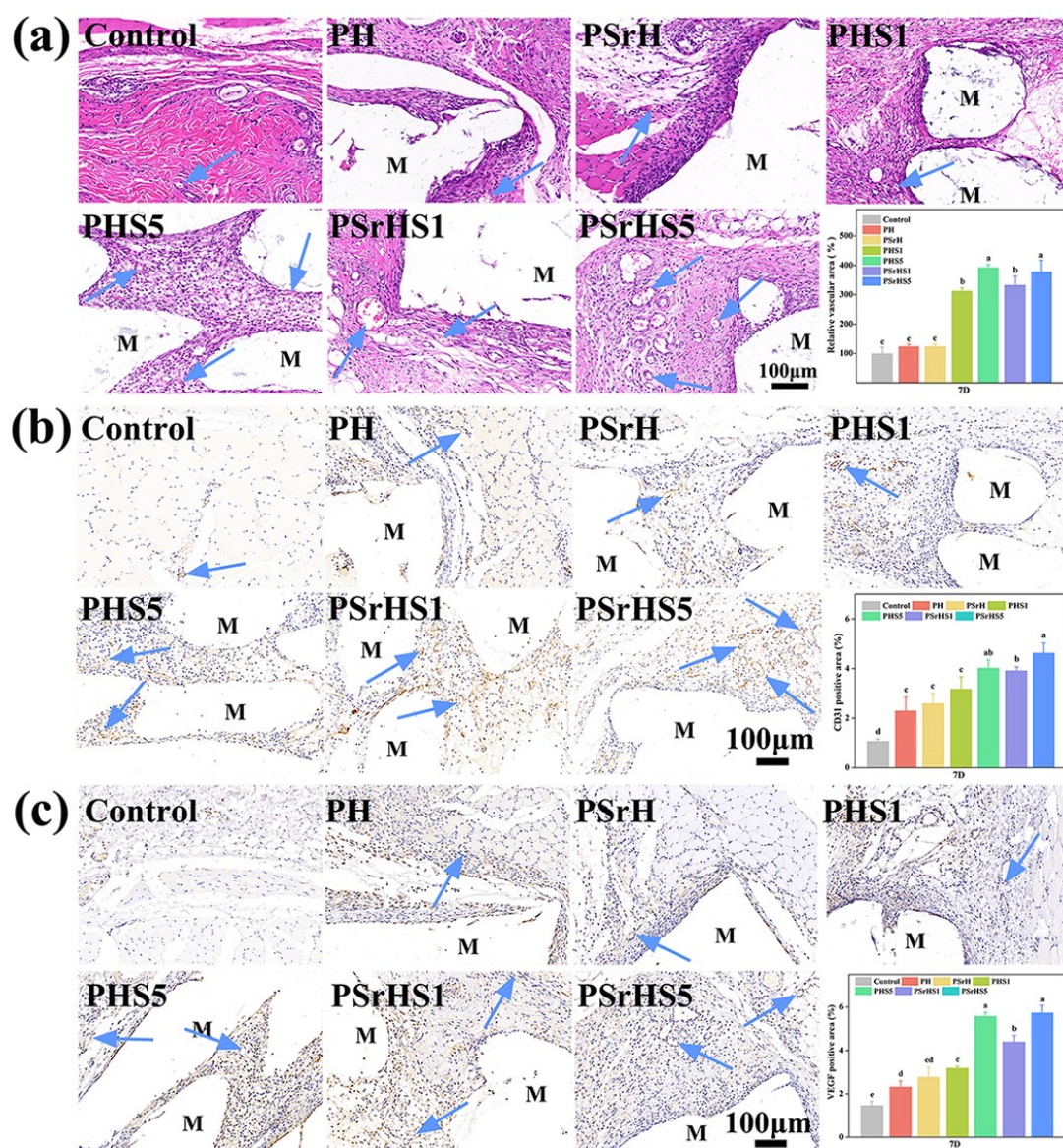


Fig. S8. Histological analysis of 3D scaffolds implanted subcutaneously in SD rats for 7 days. (a) HE

staining, immunohistochemical of (b) CD31 and (c) VEGF. n=three, M-scaffold material. The scale bar indicates 100 μ m in picture. The blue arrows in the images indicate blood vessels

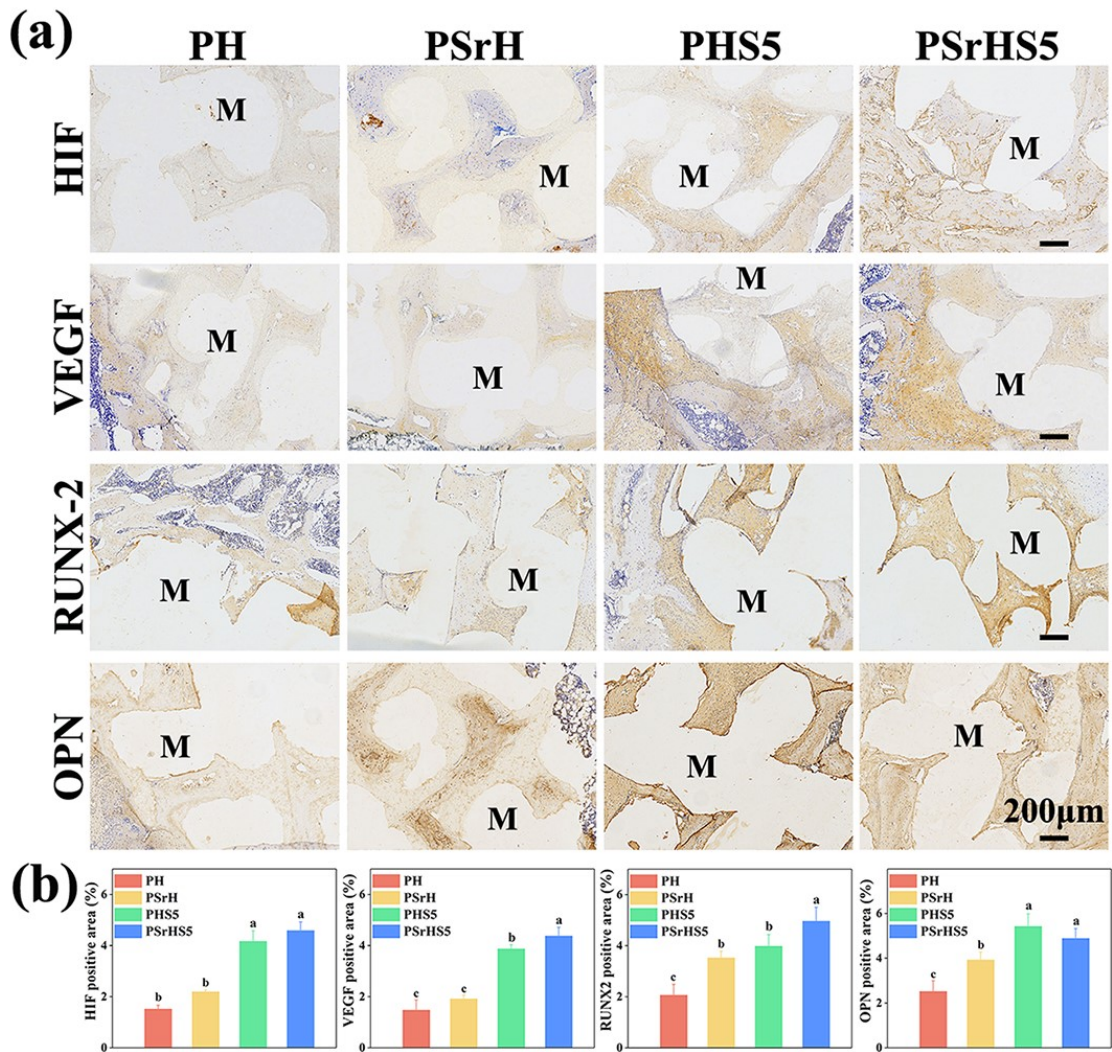


Fig. S9. Immunohistochemical stained HIF, VEGF, RUNX2, and OPN in histological sections of scaffolds and semiquantitative data after 8 weeks of implantation, M-scaffold material, n=3.

Neovascularization and new bone formation after implantation of scaffolds in the bone defect sites was further verified by IHC staining (Fig. S9) of angiogenic marker (HIF and VEGF) and osteogenic marker (RUNX2 and OPN). As shown in Fig. S8, 8 weeks after implantation, the positive area of angiogenic marker VEGF (4.38 ± 0.33 %) and osteogenic marker RUNX2 (4.97 ± 0.53 %) in the PSrHS5 group was significantly higher than that in other groups. The positive area of angiogenic marker HIF and osteogenic marker OPN in the PSrH, and PHS5 groups was obviously higher than that in PH group (Fig. S9). In brief, at eight weeks post-surgery, animals treated with PSrHS5 generated vascularized bone tissues, hence exhibiting the most-satisfying bone regeneration results compared with

the other groups. The results indicating that the synergistic effect of Sr and SIM in the scaffold significantly promoted vascularized bone regeneration.

Reference

1. M. J. Olszta, X. Cheng, S. S. Jee, R. Kumar, Y.-Y. Kim, M. J. Kaufman, E. P. Douglas and L. B. Gower, *Materials Science & Engineering R-Reports*, 2007, **58**, 77-116.
2. Xiongjun Yu, Shaobing Zhou, Xiaotong Zheng, Yu Xiao and T. Guo, *Journal of Physical Chemistry C: Nanomaterials and Interfaces*, 2009, **113**, 17630–17635.
3. X. Yu, X. Wang, D. Li, R. Sheng, Y. Qian, R. Zhu, X. Wang and K. Lin, *Chemical Engineering Journal*, 2022, **433**.
4. H. A. Rather, R. Patel, U. C. S. Yadav and R. Vasita, *Biomed Mater*, 2020, **15**, 045008.